Controlling Intermetallic Compound Growth in SnAgCu/Ni-P Solder Joints by Nanosized Cu_6Sn_5 Addition

SZU-TSUNG KAO,[1] YUNG-CHI LIN,[2] and JENQ-GONG DUH[1,2]

1.—Department of Materials Science and Engineering, National Tsing Hua University, Hsinchu, Taiwan, 300 Taiwan. 2.—E-mail address: jgd@mx.nthu.edu.tw

Nanosized Cu_6Sn_5 dispersoids were incorporated into Sn and Ag powders and milled together to form Sn-3Ag-0.5Cu composite solders by a mechanical alloying process. The aim of this study was to investigate the interfacial reaction between SnAgCu composite solder and electroless Ni-P/Cu UBM after heating for 15 min. at 240°C. The growth of the IMCs formed at the composite solder/EN interface was retarded as compared to the commercial Sn3Ag0.5Cu solder joints. With the aid of the elemental distribution by x-ray color mapping in electron probe microanalysis (EPMA), it was revealed that the SnAgCu composite solder exhibited a refined structure. It is proposed that the Cu_6Sn_5 additives were pinned on the grain boundary of Sn after heat treatment, which thus retarded the movement of Cu toward the solder/EN interface to form interfacial compounds. In addition, wetting is an essential prerequisite for soldering to ensure good bonding between solder and substrate. It was demonstrated that the contact angles of composite solder paste was $<25°$, and good wettability was thus assured.

Key words: Mechanical alloying, SnAgCu, electroless Ni-P, elemental distribution, composite solder, Cu_6Sn_5

INTRODUCTION

The solder joint plays a crucial role to provide electrical and mechanical interconnection of a silicon die to the bonding pad in an electronic system assembly. During the soldering process, solder balls react with the under-bump metallization (UBM) to form intermetallic compounds (IMCs) between the substrate and the solder. Appropriate formation of intermetallic compounds at the interface between solders and substrates ensures good metallurgical bonding. However, due to the brittle nature of the intermetallic layer, excess growth of intermetallic compounds damages joint reliability.[1,2]

In recent years, either pure metals or intermetallic compounds have been introduced into solders, forming so-called "composite solders." With the aid of reinforcement particles, the creep properties, mechanical properties, and fatigue lives of composite solders could be improved.[3,4] The morphology of IMCs formed at the solder/substrate interface was also influenced by the additives. Wu et al. showed that the particle in the composite solders strongly affected the diffusion behavior of Sn in the solder and thus also altered the IMC formation at solder/substrate interface.[5] Choi et al. reported the growth kinetics of IMCs of composite solders, and observed that Cu_6Sn_5 particles in the composite solder effectively retarded the IMC growth during long aging times.[1]

Various approaches have been used to fabricate the composite solders, such as in-situ methods,[6] gas atomization,[7] powder blending,[5] and mechanical alloying.[8] Betrabet et al. used mechanical alloying to mix SnPb solder powder and Ni_3Sn_4 intermetallic compound particles together to form composite solders.[8] Mechanical alloying, which is a high-energy milling process, is an effective way to produce composite solder powders. Homogenously dispersion-strengthened solder alloys could be formed after milling.

Development of alternative lead-free solders has recently drawn tremendous attention due to the toxicity of lead. SnAgCu is the most promising choice of lead-free solders for lower eutectic temperature, enhanced strength, improved wettability, better

(Received March 1, 2005; accepted September 2, 2005)

creep, and thermal fatigue characteristics as compared to the SnAg system.[9] Mechanical alloying (MA) is also a solid-state process to produce new alloys by high-energy ball milling at low temperatures.[6–13] Recently, a SnAgCu solder alloy was successfully produced by MA processes.[14] The SnAgCu solder paste was produced by adding flux directly into MA powders. In this study, the interfacial reaction of Ni-P layer and MA SnAgCu solders was investigated. The thickness of the IMC at the Cu_6Sn_5 containing composite solder/Ni-P interface was found to be less than that at the commercial solder joint/Ni-P interface. Similar behaviors of the IMC decrement due to the additives have also been reported in the literature.[1,5] However, detailed investigations of microstructure and elemental redistribution throughout the composite solders are limited. The aim of this study is to further investigate the detailed elemental distribution in the SnAgCu solder using x-ray composition mapping to discuss the retarding behavior of Cu_6Sn_5 in the composite solder by MA processes. In addition, the wettability of the SnAgCu solder paste by MA processes was also evaluated.

EXPERIMENTAL PROCEDURES

Different routes to produce the SnAgCu solder pastes are listed and defined in Table I. The original input powders were pure Sn, Ag, and Cu. For the composite solder, Cu_6Sn_5 was added into Sn and Ag and then mixed together to form the SnAgCu solders. In addition, the Sn3Ag0.5Cu commercial solder paste (SMIC, Senju Metal Industry Co., Tokyo, Japan) was also used for comparison. The detailed fabrication process of SnAgCu solder powders was described elsewhere.[14]

The metallization layer used was EN-8.5 wt.%P/Cu (5.5 μm)/Ti (0.1 μm)/Si. The Si wafer with 5-μm Cu on it was cut into disks of 4×6 cm^2. After cleaning ultrasonically in acetone for 6 min., acidic cleaning, and activating, the specimen was rinsed with deionized water, and then the plating process followed.

The pH value of plating solution was controlled with a 50 vol.% H_2SO_4 solution. After deposition at 85°C for 15 min., the EN-plated specimen was immediately immersed in deionized water for 2 min. and then dried with alcohol. As the UBM was plated on to the Si wafer, SnAgCu solders, including MA, composite, and commercial SnAgCu, were then applied. The RMA flux (TACFLUX, Indium Corporation of America, NY) was added directly into the solder powders at room temperature and mixed on a glass plate with a plastic spatula until a uniform mixture of flux and powder was achieved.

To probe the solder reaction and microstructure of the SnAgCu solder/electroless Ni-P assemblies, the SnAgCu solders were placed on the Ni-P UBM and then heated to 240°C for 15 min. The solder joints were sliced into individual assemblies and then mounted in epoxy. The mounted specimens were ground and polished, and microstructure analysis followed.

The interfacial morphologies between the solders and UBM were observed with a field-emission scanning electron microscope (FESEM, JSM-6500F, JEOL, Tokyo, Japan). The compositions of phases in the solder joints and elemental distribution across the joint interface were quantitatively measured with an electron probe microanalyzer (EPMA, JXA-8800M, JEOL) with the aid of a ZAF program.[15] The compositions of phases were measured and averaged for at least 10 points to ensure accuracy. The x-ray color mapping images of the solder joints were further carried out with a newly developed field-emission EPMA (FE-EPMA 8500F, JEOL).

A dynamic contact angle analyzer system (FTA200, First Ten Ångstroms, Portsmouth, VA) was used to measure the wettability of the solder pastes on electroless Ni-8.5wt.%P. The electroless Ni-P/Cu/Ti/Si substrate with solder pastes was put into the heated environment chamber. During the melting process, live images were continuously captured and transferred to the user screen. From the live images, the contact angle can be drawn and measured.

RESULTS AND DISCUSSION

Effect of Cu_6Sn_5 Nanoparticle in SnAgCu Composite Solder on the Characteristics of Solder/Electroless Ni-P Interface

Figure 1 shows the interfacial microstructure of the Sn3Ag0.5Cu solder, derived from different routes as indicated in Table I, on electroless Ni-P/Cu

Table I. Different Routes of SnAgCu Solder Pastes Employed in This Study

Route	Components	Solder Composition (wt.%)	Designation
MA process	Sn, Ag, and Cu powders	Sn3.5Ag0.2Cu Sn3.5Ag0.5Cu Sn3.5Ag0.7Cu Sn3.5Ag1Cu	MA solders
	Sn, Ag, and nano-sized Cu_6Sn_5 powders	Sn3Ag0.5Cu	Composite solders
Commercial process	Sn, Ag, and Cu powders	Sn3Ag0.5Cu	Commercial solders

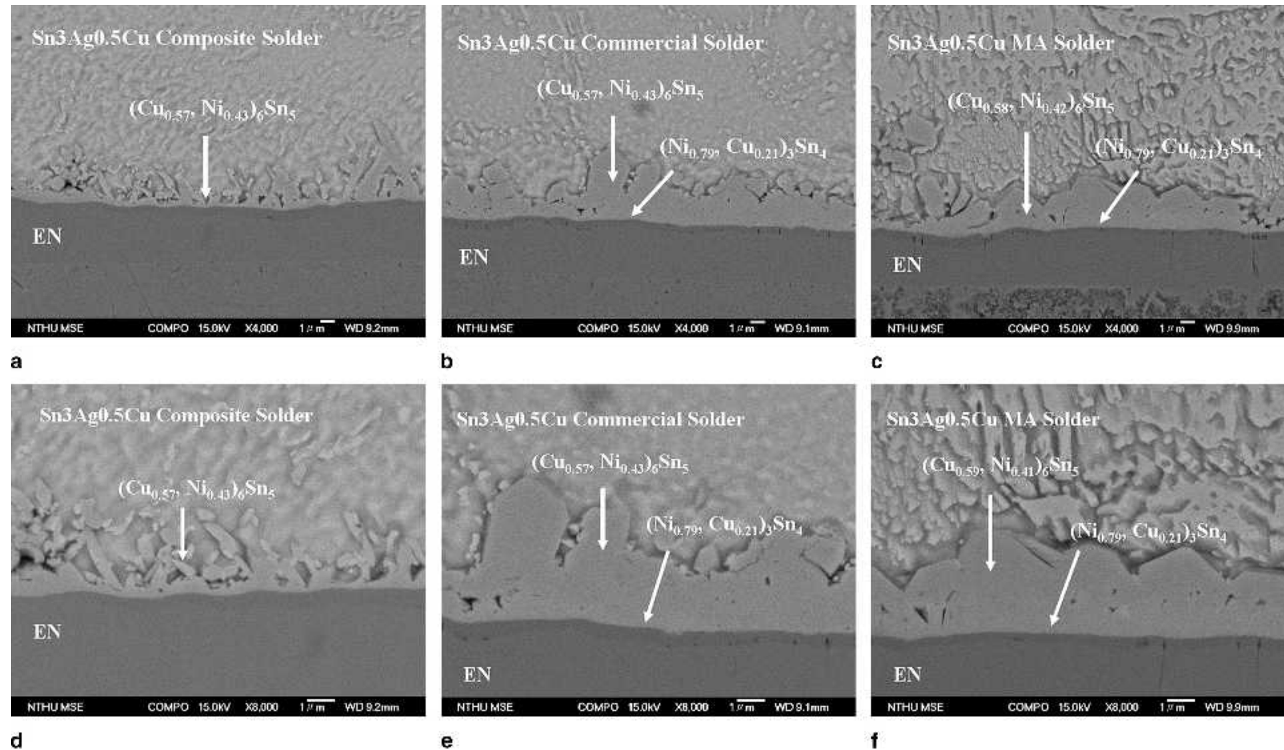

Fig. 1. Cross-sectional image of Sn-3Ag-0.5Cu solder/electroless Ni-P UBM interface after heating to 240°C for 15 min.: (a) composite solder, (b) commercial solder, and (c) MA solder. (d–f) Enlarged view of (a–c).

UBM. As reported recently,[14] the Cu_6Sn_5-doped MA solder powders exhibited a reduced size under 100 μm, and it also had an appropriate melting point. Thus, it is interesting to study the interfacial microstructure between the composite solder/UBM interfaces. Figure 1a–c show the interfacial microstructure of solder/electroless Ni-P interface, and Fig. 1d–f show enlarged views of Fig. 1a–c, respectively. As indicated in Fig. 1a for the case of Sn3Ag0.5Cu composite solder, the composition of needle-type IMC was 44.7at.%Sn-31.7at.%Cu-23.7at.%Ni. To obtain the quantitative data more accurately, the reported compositions were the average of at least ten measured points. The ratio of (Ni+Cu) to Sn was close to 6:5, and the IMC was denoted as $(Cu_{0.57},Ni_{0.43})_6Sn_5$. The compositions of IMCs for composite, MA, and commercial solder joints are listed in Table II.

The formation of the IMCs of Sn3Ag0.5Cu commercial solder joint was distinct from that of Sn3Ag0.5Cu composite solder joint. As shown in Fig. 1b, two layers were observed near the solder/electroless Ni-P interface, and the detailed quantitative analysis was measured for at least 10 points to ensure precise compositions. Upper layer was detected to be $(Cu_{0.57},Ni_{0.43})_6Sn_5$, close to the composition of needle-type IMC in the composite solder as mentioned above. The other IMC, near the electroless Ni-P layer, was detected to be $(Ni_{0.79},Cu_{0.21})_3Sn_4$.

As for the Sn3Ag0.5Cu MA solder joint, similar formation of two IMCs present at the solder/electroless Ni-P interface is illustrated in Fig. 1c. With the quantitative analysis of EPMA, the upper layer was detected to be $(Cu_{0.58},Ni_{0.42})_6Sn_5$ IMC. Another layer was considered to be $(Ni_{0.79},Cu_{0.21})_3Sn_4$.

It appears that the thickness and type of the IMC between the composite solder/electroless Ni-P interface was distinct from IMC between commercial solder/EN and MA solder/EN interface as shown in Fig. 1d–f. Thin, needle-type $(Cu,Ni)_6Sn_5$ IMC was illustrated to be formed at the composite solder/EN interface. On the contrary, IMCs of the MA solder/EN and commercial solder/EN interfaces were thicker and island-type. It is argued that the microstructure of IMC at the solder/electroless

Table II. Composition of IMCs for SnAgCu Solder Joints on Electroless Ni-P

Joint Type	IMC Type	Sn (at.%)	Cu (at.%)	Ni (at.%)
Composite solder joint	$(Cu,Ni)_6Sn_5$	44.7	31.7	23.7
MA solder joint	$(Ni,Cu)_3Sn_4$	56.8	9.2	34.0
	$(Cu,Ni)_6Sn_5$	45.6	31.8	22.6
Commercial solder joint	$(Ni,Cu)_3Sn_4$	54.4	9.6	36.0
	$(Cu,Ni)_6Sn_5$	46.2	30.5	23.3

Ni-P interface in composite solders may be influenced by Cu_6Sn_5.

In the Sn-3Ag-*x*Cu ternary phase diagram, the formation of β-Sn, Ag_3Sn, and η′-Cu_6Sn_5 after cooling from liquid phase of Sn3Ag0.5Cu alloy was revealed, as illustrated in Fig. 2.[16] In this study, β-Sn, Ag_3Sn, and η′-Cu_6Sn_5 were also found in the SnAgCu/Ni-P joint system. A more detailed x-ray color mapping was carried out to reveal the evolution of IMCs in solders. The microstructure of the composite solder joint on electroless Ni-P after heat treatment is shown in Fig. 3. The microstructure in the solders, as shown in Fig. 3a, exhibits that the primary b-Sn phase is surrounded by the eutectic network of Ag_3Sn. In fact, the ring structure of the Ag_3Sn is evident.

Figure 3b–e illustrate the x-ray color mapping of elements Sn, Ag, Cu, and Ni, respectively. According to the Sn and Ag x-ray color mapping, the presence of Ag_3Sn was evidenced. From the Cu x-ray color mapping, it appears that the distribution of Cu elements also exhibited a ring structure, as did Ag_3Sn. According to the phase diagram in the literature,[16] the Cu-rich region should be associated with the Cu_6Sn_5 IMC. The distribution of Ag_3Sn could be divided into two regions, as indicated in Sn x-ray color mapping in Fig. 3b. Region A1 shows a lower intensity of Sn and higher intensity of Ag than region A2, as illustrated in Fig. 3b and c, respectively. From Fig. 3d, there was no Cu in region A1, but it was present in region A2. It is apparent that only Ag_3Sn was observed in region A1, while both Cu_6Sn_5 and Ag_3Sn formed in region A2.

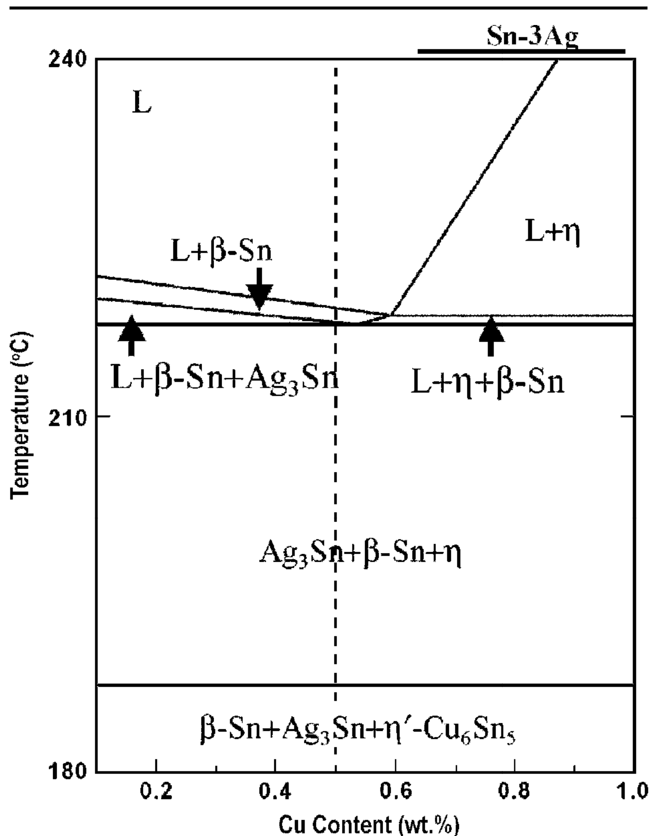

Fig. 2. Phase diagram of Sn-3Ag-xCu calculated by Thermo-Calc™.[16]

For the Sn3Ag0.5Cu commercial solder joint, the microstructure presented in Fig. 4 was distinct from that for the composite solder joint. Ag_3Sn and β-Sn phases were also found in the Sn3Ag0.5Cu commercial solder. However, it is interesting to point out that the length and thickness of the β-Sn phase increased in the commercial solder as compared to the composite solder. As shown in Fig. 3a, the size of the primary Sn is around 6–8 μm in length and 4 μm in width. In addition, as shown in Fig. 4a, the length of the Sn phase is >25 μm and the width of the Sn phase is ~ 7.2 μm, i.e., the ring structure of Ag_3Sn was more elongated in the commercial solder than it was in the composite solder. On the other hand, from the x-ray color mapping of Cu and Ni, both Cu and Ni enrichment were detected, as shown in Fig. 4d and e, respectively. Considering the higher intensity of Cu than that of Ni, the enrichment of Cu and Ni may be due to the stripping of $(Cu,Ni)_6Sn_5$ from the solder/electroless Ni-P interface.

The microstructure of Sn-3Ag-0.5Cu MA solder joint was also studied, as indicated in Fig. 5. Similar to the commercial solder joint, elongated ring structure of Ag_3Sn was observed in the solder. Besides, Cu and Ni enrichment was also detected in the solder, as shown in Fig. 5d and e, respectively.

In comparison, the Cu_6Sn_5-containing SnAgCu composite solder exhibited thin, rod-shaped $(Cu,Ni)_6Sn_5$ layers at the solder/electroless Ni-P interface, while the IMC of commercial and MA solder joints had a rounded scallop shape. In the commercial solder, a larger and longer primary Sn phase surrounded by the Ag_3Sn network was found in the solder matrix. The eutectic network was thinner and smaller as compared to that in the composite MA solder. Besides, homogeneously dispersed Cu_6Sn_5 was observed in the Cu_6Sn_5-containing SnAgCu composite solder. Due to the refined ring network of Ag_3Sn dispersion, it is believed that the mechanical properties might be enhanced.[17]

The microstructure of SnAgCu alloy was significantly affected by the additives of other elements. Ye et al. indicated that Ag_3Sn tended to be distributed homogenously throughout the microstructure of the SnAgCuB alloy.[18] The microstructure was finer in the SnAgCu alloy with B dopant. This was attributed to the fact that the presence of B provided the nucleation sites for Ag_3Sn during solidification. Only a few of Cu_6Sn_5 were found at grain boundaries within the Sn phase in the SnAgCu solder alloy, while most Ag_3Sn IMCs were located at the grain boundaries of Sn phase. In fact, the presence of Cu_6Sn_5 and Ag_3Sn phases at the boundary of β-Sn could be verified again by the x-ray color mapping and SEM. McCormack et al. also found that 1 wt.% additive of Zn element in SnAg solder alloy suppressed the formation of β-Sn dendrites, and

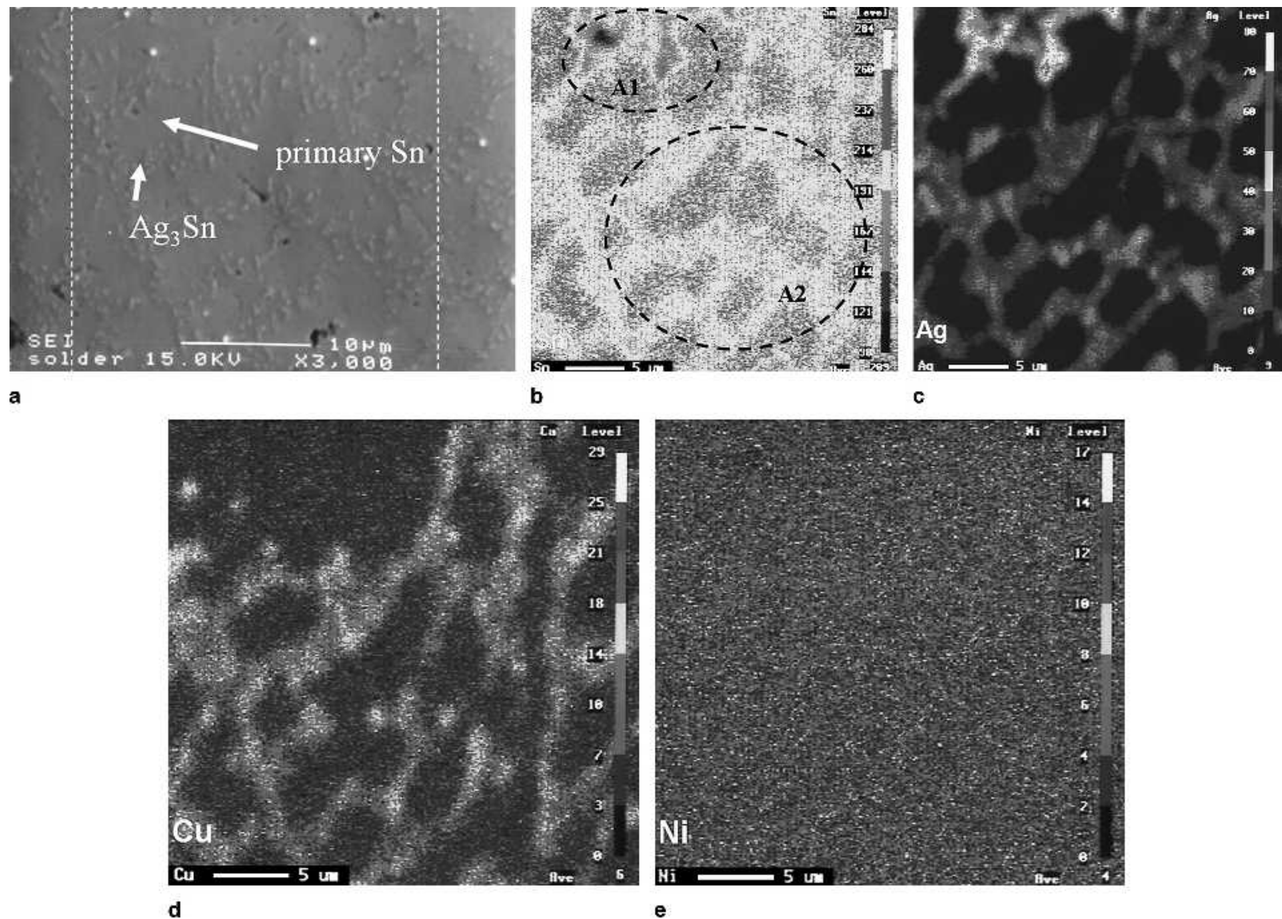

Fig. 3. Microstructure of Sn-3Ag-0.5Cu composite solder joint after heating to 240°C for 15 min.: (a) SEI image and x-ray color mapping of (b) Sn, (c) Ag, (d) Cu, and (e) Ni. The position was near the solder/electroless Ni-P UBM interface.

a fine Ag_3Sn phase distributed uniformly throughout the microstructure,[17] which is beneficial to the mechanical strength of the solder alloy.

It is well known that Cu exhibits high mobility in Sn matrix.[18] Cu, dissolved in molten SnAg solder, tended to diffuse through Sn to form Cu_6Sn_5 IMCs rather easily at the solder/substrate interface.[19] The driving force of the moving of Cu was due to the concentration difference in solders and substrate. The growth of the IMCs is affected by the additives in the solder. Wu et al. reported that the activation energy of Cu_6Sn_5 formation increased from 0.8 to 1.23 eV in the Cu_6Sn_5-containing SnPb solder joint, as compared to that of eutectic SnPb solder joint.[5] Therefore, the thickness would decrease due to the additive of Cu_6Sn_5 particles. Results in this study revealed a similar trend. Wu et al. proposed that it was attributed to the decreasing of the cross-sectional area available for Sn diffusion by additives.

Owing to the distinct fabrication process between SnAgCu composite solders and commercial solders, diverse characteristics of solders were revealed.[14] Betrabet et al. showed that Ni_3Sn_4 dispersoids, in the Ni_3Sn_4-dispersed SnPb solders fabricated by MA process, were stable at melt and maintained their original size and distribution in the solder.[8] They reported that the IMCs, dispersed in the solder matrix, would not grow during the melting process, and the refined structure was due to the pinning of these IMCs at the interface or boundaries of Sn phase. In fact, results of this study with the aid of the x-ray color mapping are in fair agreement with Betrabet's work.

As compared to the results of solder joints after heat treatment, it is concluded that the MA process provided an effective route to produce SnAgCu solders. As indicated herein, interfacial reactions and microstructure of the SnAgCu MA solder were similar to those for the SnAgCu commercial solders. In contrast to commercial or MA solders, the Cu_6Sn_5-dispersed SnAgCu solder exhibited a more refined microstructure in the solder matrix. Homogeneously dispersed Cu_6Sn_5 throughout the solder pinned at the boundary of Sn matrix, and Cu_6Sn_5 intermetallic compounds with reduced thickness <2 µm, on average, was found in the solder joints. In the literature,[8,14] it was reported that Cu_6Sn_5, <100 nm, was stable during the melting process and retained in the solder. Therefore, the dispersed Cu_6Sn_5 retarded Cu diffusion in the solder, and the amount of Cu reaching the solder/electroless Ni-P interface was also limited. MA solders or commercial solders provided fast paths for reaction of Cu with Sn at the solder/electroless Ni-P interface,

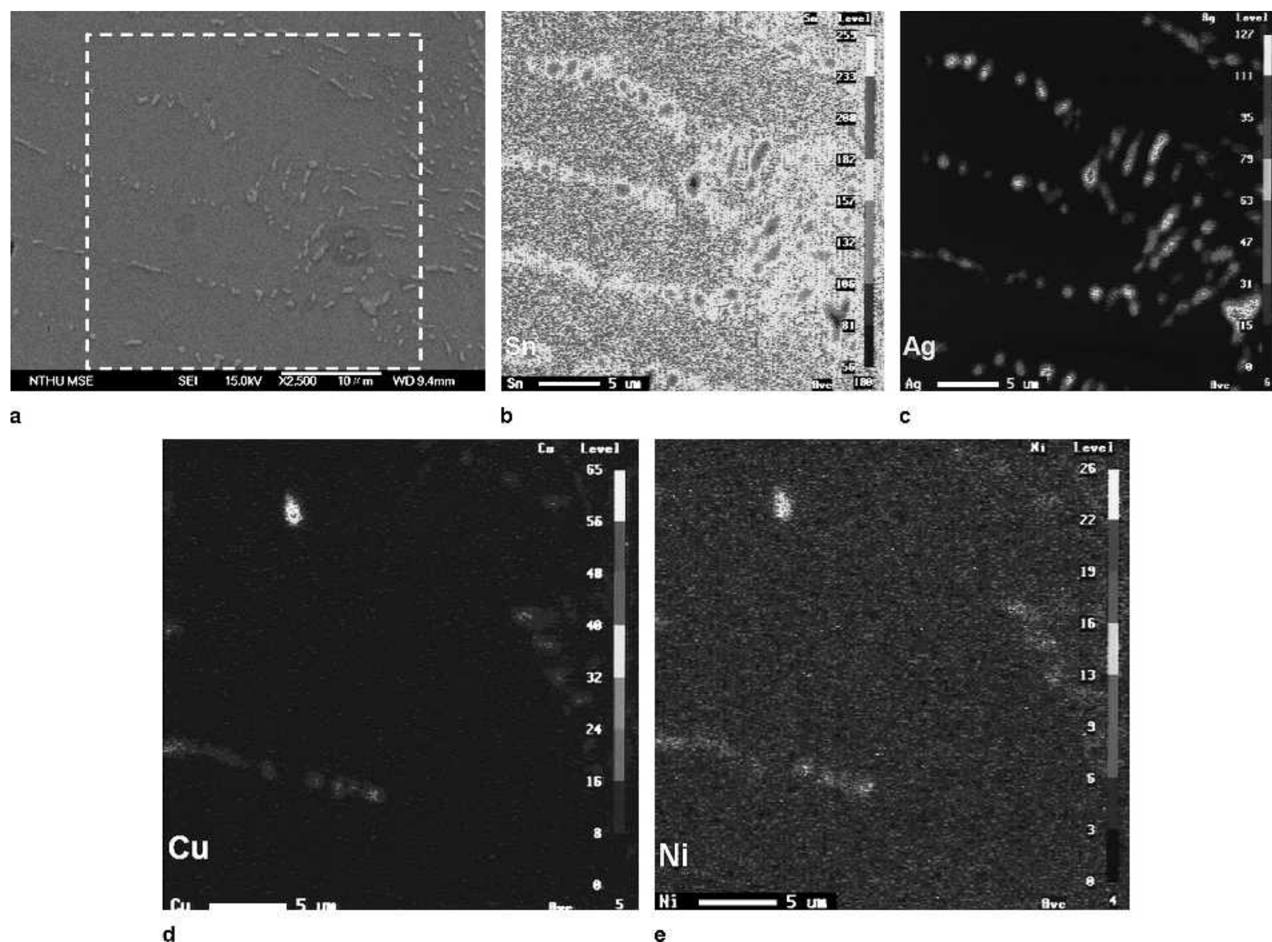

Fig. 4. Microstructure of Sn-3Ag-0.5Cu commercial solder joint after heating to 240°C for 15 min.: (a) SEI image and x-ray color mapping of (b) Sn, (c) Ag, (d) Cu, and (e) Ni. The position was away from solder/electroless Ni-P UBM interface.

causing more of an increase in thickness of Cu_6Sn_5 IMC than the MA dispersed Cu_6Sn_5 solder.

Wettability

The contact angles of three types of solder pastes on the electroless Ni-P metallization are listed in Table III. MA powders showed good wettability with contact angles less than 20°. The contact angle of the commercial solder paste was close to that of the MA solder paste. It appears that the wettability of MA solder paste was comparable to the commercial one. In addition, the wettability of the SnAgCu solder paste could be improved with the addition of Cu_6Sn_5 doping. As indicated in Table III, the contact angle of the Sn-3.5Ag-0.2Cu composite solder was smaller than that of the MA solder paste. In fact, the contact angle of both MA solder and the composite solders exhibits good wettability. In the industry, the wetting angle is ~35° between commercial solder paste and Cu UBM.[20] In this study, the wetting angle of these MA solders on EN was <30°, indicating that these MA solders could offer better wettability.

In summary, the SnAgCu solder paste fabricated by the MA process, as described above, exhibits favorable wettability. Composite solders, also fabricated by the MA process, revealed homogenously distributed and stable IMCs throughout the microstructure during melting. Thus, IMC formation at the solder/substrate interface could be retarded due to the presence of additives. With the aid of the MA process, IMC formation was controlled by mixing solder powder with other IMCs together, such as Ni_3Sn_4 nanopowders, to form new composite solders. It is expected to enhance the mechanical properties of the lead-free solders are expected to be enhanced by a controlled IMC formation and a refined solder microstructure.

Table III. Contact Angles of SnAgCu Solder Joints on Electroless Ni-P at 240°C

Solder Type	Solder Composition	Wetting Angle
MA solder paste	Sn3.5Ag0.2Cu	25°
	Sn3.5Ag0.5Cu	15°
	Sn3.5Ag0.7Cu	15°
	Sn3.5Ag1.0Cu	18°
Composite solder paste*	Sn3.5Ag0.2Cu	22°
	Sn3Ag0.5Cu	13°
Commercial solder paste	Sn3Ag0.5Cu	20°

*MA powder milled with Cu_6Sn_5 particles.

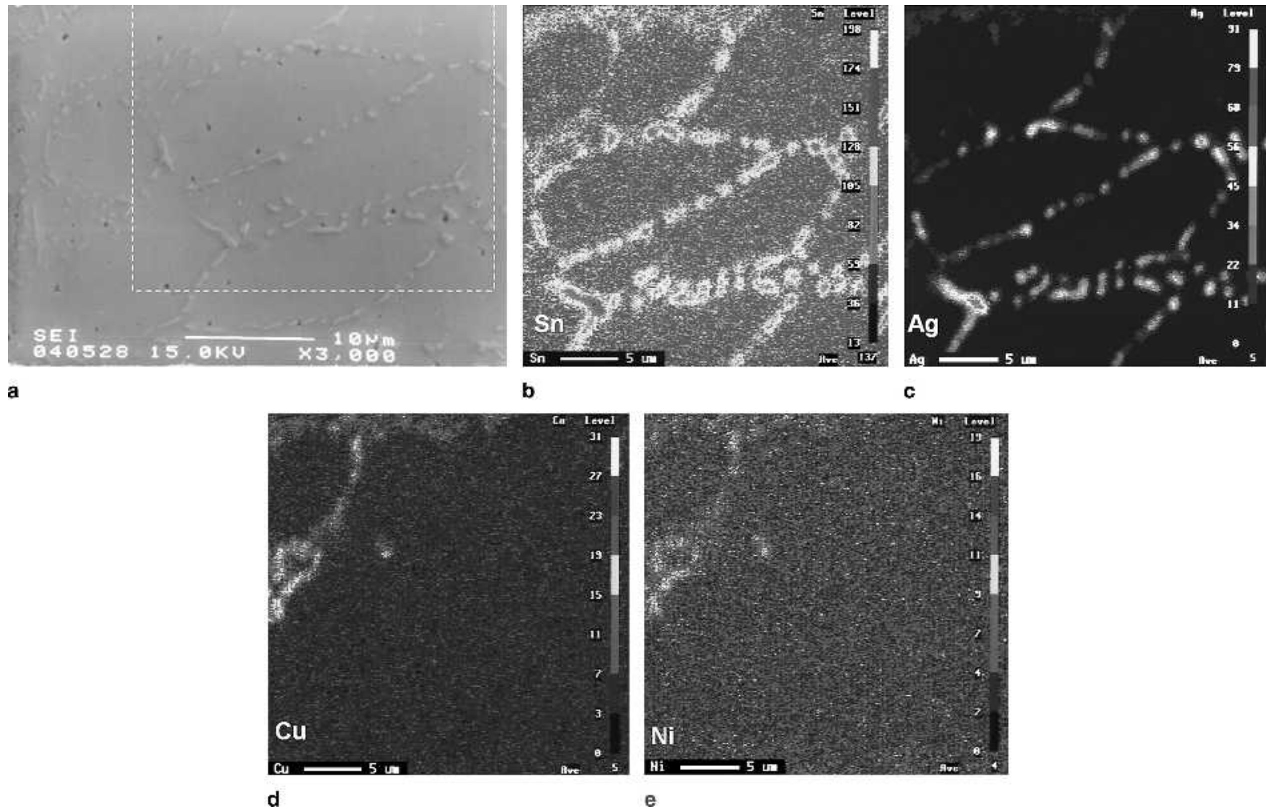

Fig. 5. Microstructure of Sn-3Ag-0.5Cu MA solder joint after heating to 240°C for 15 min.: (a) SEI image and x-ray color mapping of (b) Sn, (c) Ag, (d) Cu, and (e) Ni. The position was near the solder/electroless Ni-P UBM interface.

CONCLUSIONS

1. A composite SnAgCu solder containing Cu_6Sn_5 particles were employed in this study. After heat treatment, the interfacial reaction at solder/electroless Ni-P interface of the composite solder was distinct from that of the commercial solder and MA solders. The composite solder joints exhibited thinner $(Cu,Ni)_6Sn_5$ layers, around 1–2 μm thick, at the solder/electroless Ni-P interface, while these layers were ~3–5 μm thick in the commercial solder joint and MA solder joint. Due to the limited dissolution of Cu from Cu_6Sn_5 particles in the Cu_6Sn_5-doped composite solder, the Cu that dissolved in solders was restricted. Thus, less Cu reached the solder/electroless Ni-P interface, and IMC formation could be retarded in the composite solder joint. This provided an alternative approach to control the growth of intermetallic compound in the joint.
2. The primary β-Sn phase, surrounded by the eutectic network of Ag_3Sn, exhibited a refined microstructure in the composite solder. X-ray color mapping demonstrated that Cu_6Sn_5 in the composite solder was homogeneously distributed along with Ag_3Sn. On the other hand, the ring structure of Ag_3Sn was more elongated in the commercial solder.
3. Contact angles of MA solder joints were all <25°, indicating good wettability. It was revealed that the wettability of the SnAgCu solder paste was improved in the presence of Cu_6Sn_5.

ACKNOWLEDGMENT

Financial support from the National Science Council, Taiwan, under contracts NSC-92-2216-E007-037 and NSC-93-2216-E-007-014, is acknowledged.

REFERENCES

1. S. Choi, T.R. Bieler, J.P. Lucas, and K.N. Subramanian, *J. Electron. Mater.* 28, 1209 (1999).
2. A.J. Sunwoo, J.W. Morris, Jr., and G.K. Lucey, Jr., *Metall. Trans. A* 23, 1323 (1992).
3. J.H. Lee, D. Park, J.T. Moon, Y.H. Lee, D.H. Shin, and Y.S. Kim, *J. Electron. Mater.* 29, 1264 (2000).
4. D. Lin, G.X. Wang, T.S. Srivatsan, M.A. Hajri, and M. Petraroli, *Mater. Lett.* 53, 333 (2002).
5. Y. Wu, J.A. Sees, C. Pouraghabagher, L.A. Foster, J.L. Marshall, E.G. Jacobs, and R.F. Pinizzotto, *J. Electron. Mater.* 22, 769 (1993).
6. S.Y. Huang, J.W. Lee, and Z.H. Lee, *J. Electron. Mater.* 31, 1304 (2002).
7. R.C. Reno, M.J. Panunto, and B.H. Piekarski, *J. Electron. Mater.* 26, 11 (1997).
8. H.S. Betrabet, S.M. McGee, and J.K. McKinlay, *Scr. Metall.* 25, 2323 (1991).
9. J.H. Lau, C.P. Wong, N.C. Lee, and S.W.R. Lee, *Electronics Manufacturing: With Lead-Free, Halogen-Free and Conductive-Adhesive Materials* (New York: McGraw-Hill, 2003).
10. M.L. Huang, C.M.L. Wu, J.K.L. Lai, and Y.C. Chan, *J. Electron. Mater.* 29, 1021 (2000).

11. M.L. Huang, C.M.L. Wu and J.K.L. Lai, *J. Mater. Sci.: Mater. Electron.* 11, 57 (2000).
12. J.S. Benjamin, *Sci. Am.* 234, 40 (1976).
13. H.L. Lai and J.G. Duh, *J. Electron. Mater.* 32 (4), 215 (2003).
14. S.T. Kao and J.G. Duh, *J. Electron. Mater.* 33 (12), 1445 (2004).
15. J.I. Goldstein, *Scanning Electron Microscopy and X-ray Microanalysis* (New York: Plenum Press, 1981).
16. K.S. Kim, S.H. Huh, and K. Suganuma, *J. Alloys Compd.* 352, 226 (2003).
17. M. McCormack, G.W. Kammlott, H.S. Chen, and S. Jin, *Appl. Phys. Lett.* 65, 1233 (1994).
18. L. Ye, Z.H. Lai, J. Liu, and A. Thölén, *Soldering Surf. Mount Technol.* 13, 16 (2001).
19. S.J. Wang and C.Y. Liu, *J. Electron. Mater.* 32, 1303 (2003).
20. URL: http://www.yikst.com/Page/YIKSTE.html.